

Purification, Characterization, and Kinetic Mechanism of Cyclin D1-CDK4, a Major Target for Cell Cycle Regulation*

(Received for publication, May 6, 1998, and in revised form, July 26, 1998)

Alexandros K. Konstantinidis‡, R. Radhakrishnan, Fei Gu§, R. Nagaraja Rao||, and Wu-Kuang Yeh||

From Research Technologies and Proteins and †Cancer Research, Lilly Research Laboratories, Division of Eli Lilly and Company, Indianapolis, Indiana 46285

The cyclin D1-CDK4-pRb (retinoblastoma protein) pathway plays a central role in the cell cycle, and its deregulation is correlated with many types of cancers. As a major drug target, we purified dimeric cyclin D1-CDK4 complex to near-homogeneity by a four-step procedure from a recombinant baculovirus-infected insect culture. We optimized the kinase activity and stability and developed a reproducible assay. We examined several catalytic and kinetic properties of the complex and, via steady-state kinetics, derived a kinetic mechanism with a peptide (Rb^{ING}) and subsequently investigated the mechanistic implications with a physiologically relevant protein (Rb²¹) as the phosphoacceptor. The complex bound ATP 130-fold tighter when Rb²¹ instead of Rb^{ING} was used as the phosphoacceptor. By using staurosporine and ADP as inhibitors, the kinetic mechanism of the complex appeared to be a “single displacement or Bi-Bi” with Mg²⁺-ATP as the leading substrate and phosphorylated Rb^{ING} as the last product released. In addition, we purified a cyclin D1-CDK4 fusion protein to homogeneity by a three-step protocol from another recombinant baculovirus culture and observed similar kinetic properties and mechanisms as those from the complex. We attempted to model staurosporine in the ATP-binding site of CDK4 according to our kinetic data. Our biochemical and modeling data provide validation of both the complex and fusion protein as highly active kinases and their usefulness in antiproliferative inhibitor discovery.

The cell cycle describes a collection of highly ordered processes that ultimately result in the duplication of a cell. Cyclin-dependent kinases play an essential role in the regulation and progression of the cell cycle, including DNA duplication and accurate cell division. Cyclin D1-CDK4¹ plays a major role in the initiation of the cell cycle, the passage through the restriction point (G₀), and entry into the S-phase. The only known

target of active cyclin D1-CDK4 is the retinoblastoma tumor suppressor protein (pRb); however, other cyclin-dependent kinases such as cyclin E-CDK2 and cyclin A-CDK2 have also been shown to phosphorylate pRb in the G₁-phase and the G₁/S transition of the cell cycle. Growth suppression by pRb is closely correlated with its ability to form complexes with a number of proteins (1) through different domains of its sequence, but this function is inhibited by phosphorylation of specific serine/threonine pRb residues by cyclin-dependent kinases. Evidence supporting the idea that phosphorylation of pRb is required for G₁/S progression comes from studies of p16^{INK4}, an inhibitor of CDK4 and CDK6. This protein inhibits the phosphorylation of pRb and arrests only pRb-positive cells in the G₁-phase (2). During the cell cycle, pRb appears hypophosphorylated in the early to mid-G₁-phase and hyperphosphorylated during mitosis. Upon phosphorylation, pRb releases and activates a number of proteins such as the E2F family of transcription factors at the G₁/S transition phase (3–5), which in turn regulates the expression of several genes involved in DNA replication such as dihydrofolate reductase, thymidine kinase, and DNA polymerase α (6).

As cells enter the cycle from quiescence (G₀), one or more D-type cyclins (D1, D2, and D3) are induced and subsequently bind and activate cyclin-dependent kinases as part of the delayed early response to growth factor stimulation (7). This kinase activity, which is manifested near the mid-G₁, increases to a maximum during the G₁/S transition phase and persists through the first and subsequent cycles as long as mitogenic stimulation continues. Cyclin binding on cyclin-dependent kinase is absolutely required for kinase activity and also contributes to substrate specificity. Cyclin D1 associates predominantly with CDK4 in a complex that is subject to many levels of regulation. It has been suggested (8) that an assembly factor could be involved in stabilizing CDK4 or cyclin D1 forms compatible with the holoenzyme activation, although it may not be a part of the active complex. Cyclin D1-CDK4 is both positively and negatively regulated by phosphorylation of activating and inhibitory serine/threonine and tyrosine residues (9). On the other hand, cyclin D1-CDK4 activity can be suppressed by binding to at least two families of small inhibitory proteins such as p16 and p21 (10, 11) that might even modify their specificity or accessibility to regulators or even to substrates (12). The resulting phosphorylation pattern of pRb by the activated kinase has been studied extensively (13–21). Also, the substrate specificity and the consensus motif of the enzyme have been the subject of a detailed investigation (5) where it has been shown that cyclin D1-CDK4 and cyclin A/E-CDK2 have different phosphorylation recognition sites on pRb. Although pRb contains 16 potential CDK-mediated phosphorylation sites (Ser/Thr-Pro motifs), there are good indications that only about 10 of these residues are phosphorylated *in vivo*

* The costs of publication of this article were defrayed in part by the payment of page charges. This article must therefore be hereby marked “advertisement” in accordance with 18 U.S.C. Section 1734 solely to indicate this fact.

‡ Present address: SmithKline Beecham Pharmaceuticals, 1250 South Collegeville Rd., Collegeville, PA 19460.

§ Present address: Procter & Gamble Co., Healthcare Research Center, 8700 Mason-Montgomery Rd., Mason, OH 45040.

|| To whom correspondence should be addressed. Tel.: 317-276-7796; Fax: 317-276-9722; E-mail: Yeh_Wu-Kuang@Lilly.com.

¹ The abbreviations used are: cyclin D1-CDK4, dimeric complex; cyclin D1-CDK4, fusion protein; PAGE, polyacrylamide gel electrophoresis; MES, 2-(N-morpholino)ethanesulfonic acid; DTT, dithiothreitol; Me₂SO, dimethyl sulfoxide; pRb, retinoblastoma tumor suppressor protein; AEBSEF, 4-(2-aminoethyl)benzenesulfonyl fluoride; MS, mass spectrometry; aa, amino acid.

(18–21). Different cyclin-CDKs preferentially phosphorylate pRb at distinct sites *in vitro*, suggesting that these kinases may exert distinct effects during the cell cycle *in vivo*.

The cyclin D1-CDK4-pRb pathway is of considerable interest since its deregulation leads to reduced fidelity of cell cycle events resulting in uncontrolled proliferation and cancer (22, 23). For example, cyclin D1 amplification or overexpression appears to be a common observation of human malignancies with high frequency, such as head and neck (40%), esophageal (35%), and breast (50%) carcinoma. We anticipate that potent, selective cyclin D1-CDK4 inhibitors may have anti-tumorigenic properties by halting the growth of cancer cells that are pRb⁺, so we have been interested in developing practical novel *in vivo* and *in vitro* strategies to identify such potent compounds.

In this report, we describe the purification and extensive characterization of the biochemical and kinetic properties as well as the kinetic mechanism of this very important enzyme. This enzymatic insight in combination with an inhibitor modeling study may eventually identify critical amino acid residues of the enzyme and unique chemical entities of small molecules necessary for tight binding in the enzyme active site. In addition, we have also evaluated kinetically a fusion form of cyclin D1-CDK4, where the two subunits (cyclin D1 and CDK4) are connected with a linker peptide. The two forms of cyclin D1-CDK4, the complex and the fusion, share similar kinetic properties and mechanism, so both forms appear complementarily useful in the cell cycle inhibitor discovery.²

EXPERIMENTAL PROCEDURES

Reagents, Materials, and Cells—Staurosporine was obtained from Lilly. Small peptides (listed in Table V) were synthesized, purified, and characterized at Lilly. One batch of Rb^{ING} (aa 246–257) was purchased from Multiple Peptide Systems (San Diego, CA); purified murine Rb²¹ (aa 769–921) was from Santa Cruz Biotechnologies (Santa Cruz, CA), and [γ -³²P]ATP at 2 Ci/mmol was from Amersham Pharmacia Biotech. Other commercially available reagents are as follows: MES, Hepes, ATP, MgCl₂, DTT, EDTA, EGTA, sucrose, and trichloroacetic acid were from Sigma; AEBSEF and leupeptin were from Calbiochem; Complete Protease Inhibitor mix was from Boehringer Mannheim; microfiltration plates (phosphocellulose (MAPH) and glass fiber type C (MAFB)) were from Millipore (Bedford, MA); scintillation counting solution MicroScint 40 was from Packard (Packard Instrument Company; Meriden, CT); Poros 50HQ was from PerSeptive Biosystems (Framingham, MA); Macro-Prep Ceramic Hydroxyapatite type I (40 μ m) was from Bio-Rad; Sepharose G-25, Mono S, and Mono P were from Amersham Pharmacia Biotech. Sf9 cells were cultured in Grace's insect medium supplemented with yeastolate and lactalbumin hydrolysate (formula 91-0439BK), 1% antibiotic/antimycotic, 0.1% Pluronic F-68 (all from Life Technologies Inc.), and 10% fetal bovine serum from Sigma. pBluescript was purchased from Stratagene (La Jolla, CA), and pBlueBac was from Invitrogen.

Kinase Assay—The kinase activity assay for cyclin D1-CDK4 was carried out in a 96-well microtiter plate format measuring radioactivity incorporated in a phosphoacceptor peptide or protein co-substrate. Highly purified enzyme preparations, phosphoacceptor peptides, or Rb²¹ and [γ -³²P]ATP/ATP (as substrates) were used for the determination of the kinetic parameters by a kinase activity assay modified from that described previously (13, 25, 26). The peptide substrate was incubated in 20 mM Hepes, pH 7.5, in the presence of 14.3 mM MgCl₂, various concentrations of ATP and [γ -³²P]ATP at a final concentration of 6.077 μ Ci/ μ mol in a 65- μ l volume at 32 °C for 30 min. The reaction was initiated with the addition of 25 μ l enzyme, which was previously diluted (1:5 to 1:40) in a buffer containing 50 mM Hepes, pH 8.0, 0.1 mM DTT, 0.1 mM EGTA, 0.1 mM AEBSEF, 0.01% Triton X-100, and 10% glycerol. The reaction was stopped with 120 μ l of 10% phosphoric acid, and the plate was vortexed and 200 μ l of solution were transferred in a 96-well plate with a phosphocellulose paper filter (MAPH) and filtered through Millipore filtering apparatus with house vacuum. The plate was washed 3 times with 200 μ l of 0.5% phosphoric acid, dried with a

paper towel, and then monitored for radioactivity in a liquid scintillation counter (Packard). In addition, Rb²¹ was used as a phosphoacceptor for cyclin D1-CDK4 complex and fusion. Rb²¹ is the C-terminal portion of pRb, which spans amino acids 769–921 and could interact extensively with the enzyme and its active site, potentially in a similar fashion as the full-length pRb. When Rb²¹ was used as the phosphoacceptor protein, the assay was performed in the same way, but the reaction was stopped with 100 μ l of 25% trichloroacetic acid, followed by the addition of 25 μ l of 1 mg/ml bovine serum albumin. The plate was vortexed, 200 μ l of solution was transferred to a glass fiber plate (MABP) and counted in the same way as described above. To identify the existence of enzyme-bound intermediates, we performed the same assays in the absence of phosphoacceptor substrate to investigate possible incorporation of γ -³²P in the enzyme. One more set of assays was performed in the absence of the enzyme only, as a control which would give an estimate of nonspecific binding of [γ -³²P]ATP on the phosphocellulose filter paper. During the purification of cyclin D1-CDK4 complex, the kinase activity of chromatographic fractions was determined by using 428 μ M ATP, 3.57 μ Ci/ml [γ -³²P]ATP, and 286 μ M Rb^{ING}. For the calculation of the enzyme-specific activity, the protein concentration was determined by the Bio-Rad microassay method.

Purification of Cyclin D1-CDK4—The generation of recombinant viruses for gene cloning of cyclin D1 and CDK4 was described recently (25). The viral stocks were used to infect large scale Sf9 cultures at the indicated multiplicity of infection (27). Cells were maintained at 27 °C for 48 h and then harvested by hollow fiber concentration followed by freezing at –80 °C until further use. The purification of cyclin D1-CDK4 was performed at 4 °C. The enzyme appeared to be unstable upon storage at 4 °C, especially when the purity was low, so the purification process was carried out continuously without interruption. Whole cell pellets were suspended (1:10 ratio) in the homogenization buffer (50 mM Hepes, pH 7.5, 320 mM sucrose, 1 mM DTT, 1 mM EDTA, 1 mM EGTA, 0.1 mM AEBSEF, 20 μ g/ml leupeptin, and Complete Protease Inhibitor mixture (1 tablet/50 ml of buffer)). The cells were homogenized, using a Gla-Col homogenizer, and centrifuged at 23,700 $\times g$ for 45 min. The supernatant was filtered through a 0.22-micron filter and loaded on a Poros Q column (22 \times 1 cm) previously equilibrated with buffer A (50 mM Hepes, pH 7.5, 5 mM DTT, 1 mM EDTA, 0.1 mM AEBSEF, 20 μ g/ml leupeptin, and 10% glycerol). The column was washed with 10 column volumes of buffer A, and the protein was eluted with a linear gradient (0–1 M NaCl in buffer A). Active fractions, as analyzed by the kinase assay, were pooled together, and the salt concentration was adjusted to approximately 200 mM with buffer B (25 mM Hepes, pH 7.5, 5 mM DTT, 0.1 mM AEBSEF, and 10 μ g/ml leupeptin) and loaded onto a 15-ml hydroxyapatite column, previously equilibrated with buffer B. The column was washed with 10 column volumes of buffer B, and the protein was eluted with a linear gradient (0–500 mM potassium phosphate, pH 7.5). Active fractions were pooled and loaded on a G-25 Sepharose column for a quick exchange with buffer C (25 mM MES, pH 6.0, 5 mM DTT, 0.1 mM AEBSEF, and 5% glycerol). The desalted cyclin D1-CDK4 was loaded on a 1-ml Mono S column, previously equilibrated with buffer C, washed with 30 ml of equilibration buffer, and eluted with a linear gradient (0–1 M NaCl in buffer C). The active enzyme pool was loaded on a 1-ml Mono P column, previously equilibrated with buffer D (25 mM Hepes, pH 7.5, 2.5 mM DTT, 0.1 mM AEBSEF, and 5% glycerol), and the protein was eluted with a linear gradient (0–1 M NaCl in buffer D). Since freezing and thawing of the purified preparation decreased the specific activity, the purified enzyme was stored in aliquots at –80 °C prior to characterization and kinetic studies; under these conditions, the enzyme remained stable for months.

Purification of Cyclin D1-CDK4 Fusion Protein—The construction of the cyclin D1-CDK4 fusion protein with N-terminal (His)₆-tag and the expression of the protein in baculovirus-infected insect cells were described previously (28).² Whole cell pellets were treated similarly to those described above for the complex enzyme. During the purification the fusion enzyme appeared more stable than the complex enzyme. After cell disruption, the supernatants were dialyzed against the loading buffer (50 mM Hepes, pH 7.5, with 150 mM NaCl) and passed through a TosoHaas metal-chelating column equilibrated in the same buffer. The fusion protein was eluted with an imidazole gradient. The active fractions were pooled together, dialyzed against buffer A (loading buffer plus 5 mM DTT and 1 mM EDTA), and loaded to a Mono Q column. A linear gradient with buffer B (buffer A plus 1 M NaCl) was used to elute the protein. The last step involved concentration of the fusion protein by Amicon ultrafiltration and further purification by Superdex 200 gel filtration. Amicon Centriprep and Centricons were used to dialyze and concentrate the protein to about 10 mg/ml in buffer A for crystallization experiments (not shown).

² R. N. Rao, N. B. Stamm, K. Otto, S. Kovacevic, S. A. Watkins, P. Rutherford, S. Lemke, K. Cocke, R. P. Beckmann, K. Houck, D. Johnson, and B. J. Skidmore, manuscript in preparation.

Electrophoresis and Western Blot—The enzyme purity was analyzed by SDS-PAGE (4–20% gradient or 10% gel; ISS-Enprotech, Boston, MA). Gels were stained with Coomassie Brilliant Blue R-250, or proteins were detected by silver staining (Novex, San Diego, CA). The extent of purity was determined by scanning the stained gel with digital Imager (Alpha Innotech Corp., Oceanside, CA). Cyclin D1-CDK4 purification was also followed by Western blot using rabbit antibodies against cyclin D1 and CDK4, respectively (Santa Cruz Biotechnology, Santa Cruz, CA). Secondary antibody was peroxidase-labeled goat anti-rabbit (Vector Labs, Burlingame, CA).

Molecular Mass Determination—The gel technique of Whitaker (29) was used to estimate the molecular weight of cyclin D1-CDK4. A 25-ml Superdex 200 gel filtration column was equilibrated with several column volumes of 50 mM Hepes, pH 7.5, containing 5 mM DTT, 0.1 mM AEBSF, and 10% glycerol. Individual fractions were assayed for the kinase activity, whereas the absence of separated subunits of cyclin D1 and CDK4 was confirmed by Western blotting using anti-cyclin D1 and anti-CDK4 antibodies. The mass of the enzyme components was determined with liquid chromatography/MS on a PESCiex connected on line with a high pressure liquid chromatograph (Applied Biosystems, 140B; Foster City, CA) equipped with a microbore pump and a microbore column C8 (100 × 1 mm, Aquapore RP-300). Electrospray mass spectra were obtained using a triple quadrupole mass spectrometer (Perkin-Elmer Sciex API III; Thornhill, Ontario, Canada) equipped with a pneumatically assisted electrospray source. Samples were infused in the source of the mass spectrometer at a flow rate of 10 μ l/min using a syringe pump. Analyses were performed in the negative ion detection mode. Scans were acquired over a range of 900–2100 units in 0.1-unit intervals for a dwell time of 1 ms per interval. A total of 5–10 scans were accumulated.

Activity/Stability Optimization—By using a partially purified enzyme (Mono S eluate; approximately 75% purity), we examined the following variables for improving the enzyme activity and stability: buffer types and concentrations (Hepes, Mes, Tris, and phosphate), ionic strength (KCl), pH, DTT (1–5 mM), metal ions (Ca^{2+} , Zn^{2+} , Ni^{2+} , Mg^{2+} , Mn^{2+} , Fe^{2+} , and Co^{2+} at 14 mM final concentration), Triton X-100 (up to 0.02%), and organic solvents that were used to dissolve inhibitors (ethanol or Me_2SO up to 4% final concentration).

Kinetic Analysis—The full-length retinoblastoma protein (pRb), the physiological phosphoacceptor substrate of cyclin D1-CDK4, contains 16 potential phosphorylation sites. There is strong evidence (14) that about 10 of them are phosphorylated *in vivo*. Therefore, using pRb as a substrate, it would be difficult to extract any meaningful conclusion about the phosphorylation process since each one of these phosphorylation sites should be recognized as a unique substrate for the enzyme. On the other hand, the commercial cost for multi-milligram quantity was estimated to be very high; thus, it appeared impractical in acquiring any extensive kinetic data with this protein substrate. Alternatively, we examined the mechanistic question indirectly by performing steady-state kinetics with a simple peptide (Rb^{ING}) that contains only one phosphorylation site (5) and by correlating qualitatively these kinetic data with those obtained with a more physiologically relevant phosphoacceptor protein (Rb^{21}). In the former case we ignored the presumably extensive interactions between the enzyme and the substrate and focused on the phosphorylation event under conditions of limited electrostatic interactions. The kinetic data were modeled according to the following Equation 1.

$$1/v_0 = \{K_m^{\text{ATP}}/V_{\text{max}}[\text{ATP}]\} + \{K_m^{\text{Rb}^{\text{ING}}}/V_{\text{max}}[\text{Rb}^{\text{ING}}]\} + \{K_s/V_{\text{max}}[\text{Rb}^{\text{ING}}][\text{ATP}]\} + 1/V_{\text{max}} \quad (\text{Eq. 1})$$

where [ATP] and $[\text{Rb}^{\text{ING}}]$ represent the concentrations of the substrates and K_m^{ATP} and $K_m^{\text{Rb}^{\text{ING}}}$ are the Michaelis constants (30). Kinetic data were processed by unweighted iterative nonlinear least squares fitting of initial velocities as a function of substrate concentration. The kinetic parameters obtained by fitting the data points to rectangular hyperbolic plots were then used to plot the initial velocity pattern in linear double-reciprocal form as shown in all figures. Kinetic constants were derived from the secondary plots of the best-fit parameters from the primary data patterns. The result was the same when the data were all fitted in the equation describing a bi-substrate enzyme catalysis. Inhibition types were assigned by considering the statistical significance of the difference between intercept and/or slope values of double-reciprocal plots from experiments in the presence and absence of the inhibiting agent. Kinetic parameters were estimated by using the nonlinear least squares statistical analysis software package JMP (SAS; Cary, NC) run on a Power Macintosh personal computer. The graphs were made using

a graphics program KaleidaGraph (Synergy Software, Reading, PA). In our calculations, we assumed that the purified enzyme was fully active as determined above.

For the inhibition experiments with staurosporine, a stock solution of 500 μ M staurosporine in Me_2SO was made and further diluted with 10 mM Hepes, pH 7.0, to a stock solution of 200 μ M final concentration. This stock solution was adjusted to the desired concentrations for inhibition studies in the range of 200 nM to 1 μ M with buffer Me_2SO , 10 mM Hepes, pH 7.0, in a ratio 4:6.

Modeling of Cyclin D1-CDK4: Staurosporine in ATP-binding Site—As there was no three-dimensional structure of human CDK4 available, this was determined by homology modeling (31, 32) using the known homologous structures of cyclic AMP-dependent kinase (33), mitogen-activated protein kinase ERK2 (34), and CDK2 (35) (1apm.pdb, 1erk.pdb, and 1aql.pdb from Brookhaven National Laboratory, Upton, NY, data base (36)). The software Homology (from Biosym Technologies, now a part of Molecular Simulations Inc., San Diego, CA) and the program “Modeller” (37) available through Quanta (Molecular Simulations Inc., San Diego, CA) were used to obtain the three-dimensional model. The program Homology was used to obtain the sequence alignments using the conserved structural regions in the three proteins. The sequence alignment thus obtained was used in Modeller to obtain the final model for CDK4. Staurosporine was modeled using its absolute configuration (38) and docked into the active site of CDK4 using the structure of CDK2-staurosporine complex (39).

This model is based on the experimental observations discussed below, that staurosporine inhibits the catalytic activity of CDK4 by competing for binding with the co-substrate ATP. The objective of this modeling was to explore the interacting residues in CDK4 with staurosporine. This modeling study relied on the analysis of the CDK2-staurosporine complex as provided in the crystal structure as referred to above. It is to be noted that Furet *et al.* (39) correctly predicted the common binding mode of ATP and staurosporine where the lactam amide nitrogen mimics the 6-amino nitrogen of ATP. Energy minimization of the complex was performed using CHARMM force field (40) as implemented in Quanta to relieve the short contacts.

RESULTS

Cyclin D1-CDK4: Activity/Stability Improvement—By using partially purified enzyme, we optimized a number of factors such as buffer type, pH, ionic strength, and other factors that might affect the activity and stability of cyclin D1-CDK4. The best buffer appeared to be Hepes. The kinase activity was optimal in 50 mM Hepes buffer, pH 7.0, and it was 3.5 times higher than in phosphate buffer at the same pH and ionic strength. Probably phosphate depletes Mg^{2+} , which is important for the enzyme function since it stabilizes the transition state of ATP during hydrolysis of the γ -phosphate. Although the activity was optimal at 50 mM Hepes, the complex appeared to be more stable over time in 10–20 mM Hepes. In Tris buffer, pH 7.8, the activity was 2.2 times higher than in phosphate at pH 7.8 but was still 1.6 times lower than that in Hepes at the same pH. Mg^{2+} was the preferred metal ion, and substitution with Mn^{2+} at the same concentration resulted in 28% activity loss. The other metal ions failed to show any enzyme activity. DTT up to 5 mM had no effect on the activity; however, it improved the enzyme stability probably because of the existence of an oxidizable cysteine in the enzyme. Triton X-100 at 0.02% was required for maximal activity and, in its absence, only 58% activity remained. In the presence of Me_2SO (4% final concentration), which was used to dissolve inhibitors that were not water-soluble, the activity increased slightly (~10%).

Cyclin D1-CDK4 Complex and Fusion Proteins: Purity and Identity—As summarized in Table I, cyclin D1-CDK4 complex was purified 13-fold at 4% activity recovery from the crude extract by a four-step procedure including Poros Q, hydroxyapatite, Mono S, and Mono P. Based on SDS-PAGE (Fig. 1A), the enzyme complex was near homogeneous, at least 87% pure, with a molar ratio of 1:1 for the two subunits. Multiple chromatographic forms of cyclin D1-CDK4 were observed, especially during the first two steps, and they caused broadening of

TABLE I
Purification of cyclin D1-CDK4

Step	Total activity	Total protein	Specific activity	Recovery
	<i>cpm</i>	<i>mg</i>	<i>cpm/min-mg</i>	<i>%</i>
Crude extract	335,362,800	692	16,160	100
Poros Q eluate	182,170,880	165	36,820	54
Hydroxylapatite eluate	74,624,220	19	134,125	22
Mono S eluate	22,991,840	5.4	142,984	7
Mono P eluate	12,064,520	1.96	205,179	4

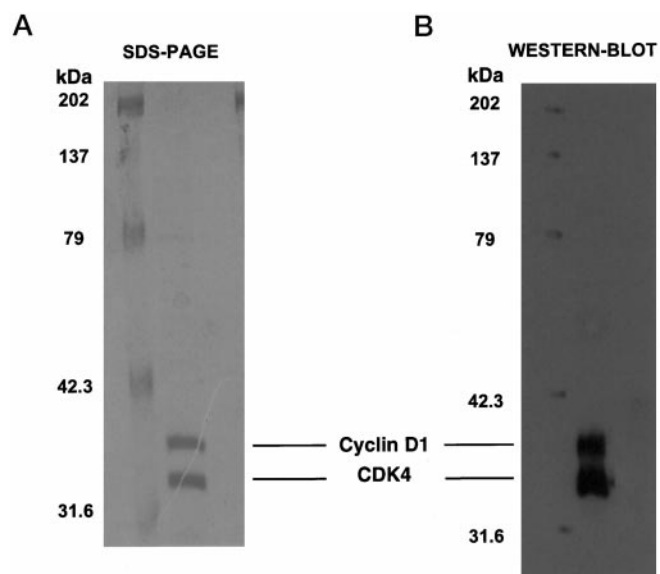


FIG. 1. **SDS-PAGE and Western blot of purified cyclin D1-CDK4 complex.** A, the purified enzyme (10 μ g) was loaded on a 4–20% gel, and the proteins were stained with Coomassie Blue. B, the purified enzyme (10 μ g) was loaded on a 4–20% gel, and the Western blot was probed with anti-cyclin D1 and anti-CDK4 antibodies and then developed with enhanced chemiluminescence (ECL; Amersham Pharmacia Biotech).

the activity peaks. This heterogeneity could be due to different post-translational processing from the baculovirus expression system (41), N-terminal residue removal or modification, or due to the tight binding of the enzyme to other cellular proteins that are structurally similar to the physiological substrate (pRb) or kinase inhibitors. The actual activity recovery at each of the first three steps was quite high (>60–90%) but, due to the enzyme micro-heterogeneity, we pooled only the fractions with the highest specific activity for further purification. The specific activity of the final preparation was 11 μ mol of Rb^{ING} phosphorylated per min-mg of enzyme when both substrates are at saturating concentrations.

Western blot using the specific cyclin D1 and CDK4 antisera (Fig. 1B) confirmed the molecular identities of the cyclin D1 and CDK4 subunits. The molecular weight of the purified complex could be determined from the mass of the two subunits by LC-MS: 33,731 for cyclin D1 (theoretical 33,730) and 33,858 for CDK4 (theoretical 33,854) which accounts for a single phosphorylation and a single acetylation of the latter protein. Edman sequencing of CDK4 showed that the N terminus was blocked, consistent with the possible single acetylation. There was also a minor (less than 3%) possibly CDK4 component, which appeared to be acetylated but dephosphorylated. Trypsin digestion of the purified enzyme complex followed by peptide sequencing by MS/MS identified a number of expected cyclin D1 and CDK4 peptides. The molecular mass of the active enzyme complex was determined by analytical gel filtration (Superdex 200) to be 67-kDa, which implies that no other protein factor (e.g. the “assembly factor”) is required for full kinase activity of

the enzyme. As determined by both Western blotting and kinase activity assay, no individual cyclin D1 or CDK4 subunits or other oligomers with higher molecular weight than the dimer were eluted from the gel filtration. This implies that the dimer appears to be the functional molecular entity of the kinase.

Freshly purified cyclin D1-CDK4 fusion protein appeared homogeneous as a single band on silver-stained SDS-PAGE with apparent molecular mass of 75 kDa (Fig. 2A). It also appeared as a single species by mass spectrometry with molecular mass of 72.57-kDa. If the purified enzyme sample was stored at 4 °C for a long time or frozen at –80 °C and thawed prior to the gel filtration step, the monomeric cyclin D1-CDK4 fraction from the Superdex 200 column in comparison to the freshly purified protein decreased, whereas the high molecular weight complexes (aggregated forms) became increased (Fig. 2B). The aggregation behavior of the cyclin D1-CDK4 fusion protein was also investigated using native gel electrophoresis and Western blot. The freshly purified protein appeared as a single band in SDS-PAGE, but upon prolonged storage at 4 °C, it generated a ladder of various high molecular weight complexes on the native gel (not shown). Therefore, all the kinetic experiments with the fusion protein were carried out with a freshly purified enzyme.

Cyclin D1-CDK4: Reproducible Kinase Assay—By using the purified cyclin D1-CDK4 complex and the fusion enzyme, we developed a highly reproducible kinase assay; the optimized conditions are shown in Table II. This assay was useful with Rb^{ING} and other small peptides as well as with the more physiologically relevant phosphoacceptor substrate, Rb²¹ (a C-terminal portion of pRb linked to a glutathione *S*-transferase tag). With this optimized assay, for the enzyme complex and partially for the fusion protein, we were able to determine the kinetic constants (K_m and V_{max}), to evaluate ADP and staurosporine as a product and a dead-end kinase inhibitor, respectively, and to establish the kinetic mechanism of the enzyme, as described below.

Cyclin D1-CDK4: General Kinetic Mechanism—The initial velocities for the cyclin D1-CDK4 were determined by using Rb^{ING} as the phosphoacceptor. When Mg^{2+} -ATP was the variable substrate with different concentrations of Rb^{ING} as the fixed substrate, an intersecting pattern of initial velocities was obtained for the reciprocal plots (Fig. 3A). The overall kinetic behavior of the enzyme appears compatible with that of “single displacement” (also known as “sequential” or “Bi Bi”) mechanism. The kinetic data, which were modeled according to Equation 1 (under “Experimental Procedures”), are shown in Table III. The close fit of the modeled lines to the data supports the use of this equation. The concentration of Mg^{2+} was sufficiently high that essentially all ATP was present as Mg^{2+} -ATP at this pH and ionic strength (42). On the other hand, the primary plots of $1/v$ versus $1/Rb^{ING}$ showed a pattern of lines that converge on the *y* axis (data not shown), which is compatible with competitive activation by ATP and indicates that it may be an “Ordered Bi Bi” mechanism with ATP as the leading substrate. From the replots of the intercepts and the slopes (Fig. 3, B and C) of the primary plot versus the concentration of

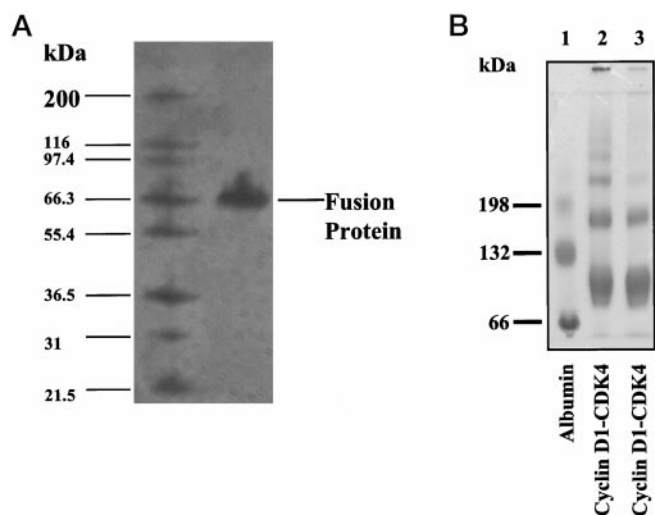


FIG. 2. **SDS-PAGE and native-PAGE of purified cyclin D1-CDK4 fusion protein.** A, the Superdex 200-purified protein (15 μ g) was loaded on a 4–20% gel, and the protein was stained with Coomassie Blue. B, the purified enzyme (20 μ g) from two preparations (non-reducing, lane 2; and reducing, lane 3) was loaded on a 4–20% gel under non-denaturing conditions, and the proteins were stained with Coomassie Blue.

TABLE II
Cyclin D1-CDK4, enzymatic assay

Optimized activity conditions	
Enzyme	Highly purified (~90%) D1/K4 dimer
Substrate	(a) ≥ 6 mM ATP (saturating) (b) ≥ 1.5 mM Rb ^{ING} (saturating)
Mg ²⁺	14.3 mM
Buffer	50 mM Hepes, pH 7.0
Me ₂ SO	4%
DTT	1 mM
EGTA	1 mM
Triton X-100	0.02%
Temperature	30 °C
Reaction time	30 min

the phosphoacceptor, we calculated the kinetic parameters of the kinase reaction (Table III).

The same set of experiments was performed in the same way for the cyclin D1-CDK4 fusion protein in order to determine whether this form and the dimeric complex operate by the same kinetic mechanism and to determine the kinetic parameters of the fusion form for comparison. The same kinetic mechanism was observed for the fusion protein (not shown). The specific activities of the two enzymes appeared to be similar (Table III), indicating that the connecting peptide did not significantly affect the activity of the fusion protein. The binding constants of ATP and the small peptide Rb^{ING} for the fusion protein also appeared to be similar to those of the dimeric complex (Table III).

Cyclin D1-CDK4: Specific Kinetic Mechanism—The initial velocity pattern (Fig. 3) and the lack of isotope exchange between Mg²⁺·ATP and the enzyme indicate that the kinetic mechanism of cyclin D1-CDK4 is sequential, *i.e.* both substrates are added to the enzyme prior to the release of the first product. However, these studies do not differentiate whether the addition of the substrates, the release of products, or both follow an obligatory order or a random fashion. Our inhibition experiments were designed to determine the order of substrate entry and product discharge for both enzymes. Staurosporine was known to be a potent competitive inhibitor of a large number of protein kinases (43). As indicated by the pattern of inhibition in the reciprocal plot (Fig. 4A) when the dimeric

complex was used with ATP as the varied substrate, there was a marked slope effect with no change in the intercept, indicating a competitive inhibition. The initial velocity pattern with Rb^{ING} as the varied substrate showed that staurosporine was a non-competitive inhibitor of Rb^{ING} (Fig. 4B). The limitation of this experiment was caused by phosphoacceptor-peptide substrate inhibition, and thus we could not achieve saturating Rb^{ING} substrate concentrations. So we solved the problem by performing multiple experiments and confirming both the intercept and the slope effects. If Rb^{ING} was the first substrate to enter the enzyme, staurosporine would still be a competitive inhibitor of ATP, but it would appear as uncompetitive of Rb^{ING}. This indicates that staurosporine competes with ATP for binding the same binding site. The results obtained with staurosporine as a dead-end inhibitor suggest that ATP binds first and Rb^{ING} binds second in an ordered manner. The same set of inhibition experiments was performed for the fusion form of cyclin D1-CDK4, and the results both qualitatively and quantitatively appear to be the same as for the complex enzyme (Table IV). This shows that the linker peptide that connects the two subunits does not seem to affect the kinetic properties of the enzyme when the phosphoacceptor substrate is a small peptide and probably is not involved in the phosphoacceptor binding.

To determine the order of release of the products, Mg²⁺·ADP was used as a product inhibitor of the dimeric enzyme. If Mg²⁺·ADP were the last product released with Mg²⁺·ATP as the leading substrate, Mg²⁺·ADP would be competitive with respect to Mg²⁺·ATP, since they compete for the same active site. On the other hand, if Mg²⁺·ADP were the first product released, it would be uncompetitive with respect to Mg²⁺·ATP when Rb^{ING} was near saturation but noncompetitive if the concentration is sub-saturating. The data presented in Fig. 4C clearly show that the pattern of inhibition was uncompetitive with $K_i = 2$ mM, thus consistent with Mg²⁺·ADP as the leading product. Therefore, it appears that the phosphorylated protein is released last. The inhibition results with Mg²⁺·ADP are consistent with a mechanism that Mg²⁺·ATP binds first and the phosphorylated peptide is released last (Scheme 1).

Cyclin D1-CDK4: Phosphoacceptor Effect on Kinetic Properties—By having established the kinetic mechanism of the dimeric complex with the small peptide, we performed several preliminary experiments to examine qualitatively the interaction of the complex enzyme with a more physiologically relevant substrate, and as such we picked Rb²¹. Since it is known that glutathione *S*-transferase is not phosphorylated by cyclin D1-CDK4 (44), we could use GST-Rb²¹ for the kinetic studies expecting that the contribution of the glutathione *S*-transferase domain to the enzyme-substrate interaction may be insignificant. This portion of pRb contains Ser-780, which has been shown (4) to be phosphorylated in the early G₁-phase during the cell cycle specifically by cyclin D1-CDK4 but not by cyclin A/E-CDK2, so this pRb portion is in fact relevant for the physiologic function of the enzyme. Cyclin D1-CDK4 phosphorylated Rb²¹ following hyperbolic kinetics; however, our inability to reach saturation concentrations of Rb²¹ limits our interpretation of the general interaction between the enzyme and this substrate. When Mg²⁺·ATP was used as the variable substrate with Rb²¹ as the fixed co-substrate, we did get saturation kinetics of ATP. Interestingly, for the complex enzyme, the apparent K_m^{ATP} with Rb²¹ as the phosphoacceptor was 10 μ M or 130-fold lower than the K_m^{ATP} with Rb^{ING} as the substrate. The phosphorylation process of Rb²¹ by cyclin D1-CDK4 is still under further investigation, so this apparent K_m value and a comparison with the K_m^{ATP} in the presence of Rb^{ING} can only be interpreted in a qualitative manner. Apparent K_m^{ATP} does not

FIG. 3. **Initial velocity and secondary patterns for cyclin D1·CDK4 complex.** A, the initial velocity pattern for cyclin D1·CDK4 was determined with ATP as the varied substrate at the following concentrations of Rb^{ING}: 0.21 mM (●), 0.29 mM (○); 0.49 mM (×); and 1.47 mM (■). The initial velocity (v) is defined as the [³²P]PO₄ incorporated in Rb^{ING} in cpm per 30 min of reaction. B, the secondary plot was from the primary intercepts *versus* reciprocal Rb^{ING} concentration. C, the secondary plot was from the primary slopes *versus* reciprocal Rb^{ING} concentration. Further details are described under "Experimental Procedures."

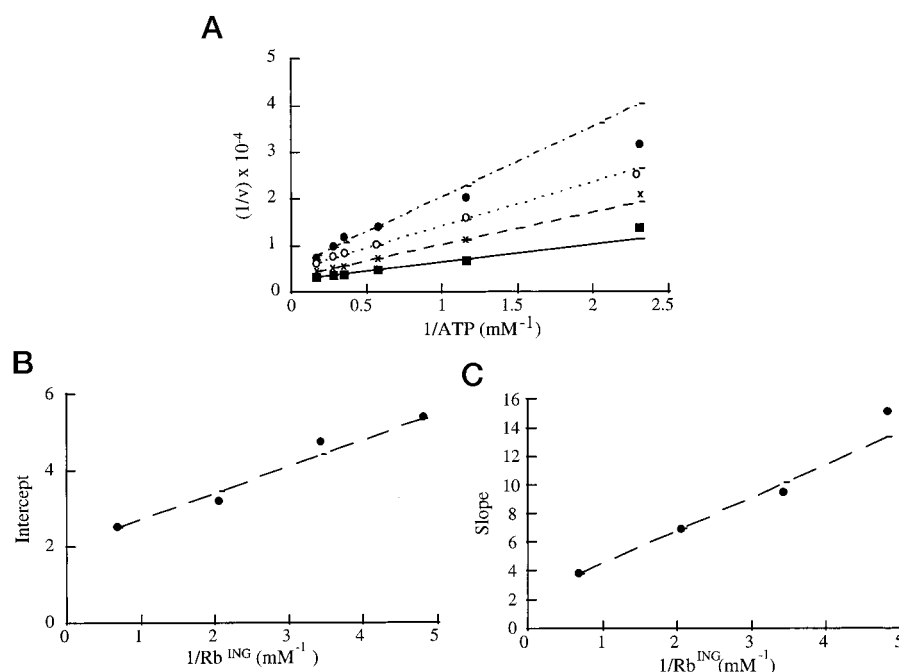


TABLE III
Cyclin D1/CDK4, kinetic parameters

Phosphoacceptor substrate Rb ^{ING} , complex cyclin D1 · CDK4	Phosphoacceptor substrate Rb ^{ING} , fusion cyclin D1·CDK4
$V_{max} = 11 \mu\text{mol/min} \cdot \text{mg}$	$V_{max} = 8 \mu\text{mol/min} \cdot \text{mg}$
$K_m^{ATP} = 1.3 \pm 0.1 \text{ mM}$	$K_m^{ATP} = 1.7 \pm 0.1 \text{ mM}$
$K_m^{Rb^{ING}} = 350 \pm 15 \mu\text{M}$	$K_m^{Rb^{ING}} = 330 \pm 20 \mu\text{M}$

describe the phosphorylation of a single serine/threonine residue of Rb²¹ but instead represents a cumulative effect of all serine/threonine residues that are phosphorylated by cyclin D1·CDK4. The tighter binding of ATP to the enzyme can be explained by a conformational change in the enzyme that Rb²¹ may induce upon binding to the active site. This conformational change may lead to further stabilization of the enzyme-ATP complex or probably a better alignment of the β - γ phosphate bond of ATP into a position that favors nucleophilic attack by the phosphoacceptor substrate (45). An ATP inhibition that was observed when Rb^{ING} was the phosphoacceptor was not detected in the presence of Rb²¹; no inhibition was detected at an ATP concentration that was 40 times that of the K_m . By using the same concentration of fusion enzyme as that for the complex and the fixed concentration of Rb²¹, we performed the same kinetic experiment and obtained a K_m^{ATP} of 36 μM for the fusion form, 3.6-fold higher than that of the complex form. This is a clear indication that, although both complex and fusion forms appear to have the same kinetic properties in the presence of small phosphoacceptor peptide, there is a difference in ATP affinity when the phosphoacceptor substrate is physiologically relevant, close in length to the full-length pRb. Our kinetic data suggest that, overall, Rb²¹ interacts more extensively with the holoenzyme, and the conformational change is presumably the result of this tighter interaction. The linker peptide not only affects the physiological properties of the enzyme such as aggregation but also the kinetic properties in a subtle way.

Substrate Specificity—We have shown so far that the complex and fusion forms of cyclin D1·CDK4 appear to operate by the same kinetic mechanism whether the substrate is a small peptide or a larger portion of the C terminus of pRb, which is

the physiologically relevant substrate. We also determined the kinetic parameters of the two enzyme forms using several small peptides that contained potential phosphorylation sites (serine and/or threonine) of pRb. Both enzymes showed highly similar activities toward the six small peptides, and they also had very similar kinetic constants toward three additional small peptides (Tables V and VI).

CDK4: Modeling of Staurosporine in the ATP-binding Site of CDK4—The essential interactions, hydrogen bonding and non-bonded contacts, are depicted in Fig. 5 (using Ligplot (46)). As CDK2 and CDK4 have high sequence homology (45.7% sequence identity and 71.6% similarity using Smith-Waterman alignment method (47) with BLOSUM62 matrix), and also they are functionally similar enzymes, the active site of CDK4 is not very different from that of CDK2. Nevertheless, there are some subtle but quite definite differences in the surrounding residues of the active site. All four hydrogen bonds as observed in the CDK2-staurosporine complex are seen in the CDK4-staurosporine model. The proximity of Asp-99 in CDK4 (equivalent to Asp-86 in CDK2) to the nitrogen N-4 (methylamine) attached to the glycosyl group of staurosporine tempted us to treat the interaction between the two as a salt bridge rather than a hydrogen bond. One of the major differences between CDK2 and CDK4 active site residues is the His-95 whose corresponding residue in CDK2 is Phe. The interaction between this residue and staurosporine does not seem to be significant except providing an opportunity to donate a hydrogen bond to the oxygen of the lactam part of staurosporine (His-95 ND1—O5) in circumstances when the existing hydrogen bond between Val-96 backbone nitrogen and the oxygen of the lactone breaks. Equivalent hydrophobic interactions between staurosporine and CDK2 could be accounted for between staurosporine and CDK4. It is also seen from the model that the following residues Ile-12, Val-20, Ala-33, Val-72, Phe-93, Glu-94, His-95, Val-96, Asp-97, Asp-99, Lys-142, Glu-144, Asn-145, Leu-147, Asp-158 of CDK4, being in a more dynamic environment, could be potentially involved in interacting with staurosporine either through backbone interactions, hydrogen bonding, and/or through forming salt bridges. It is possible for staurosporine to have similar, if not identical, kind of interactions with CDK4 as it has been reported to have with CDK2, as

FIG. 4. Inhibition of cyclin D1-CDK4 complex by staurosporine and ADP. A, Rb^{ING} was held constant at 1 mM (~3× K_m^{Rb^{ING}}); ATP was used as the varied substrate and staurosporine concentrations were 0 (●), 250 nM (○), and 500 nM (×). B, ATP concentration was held constant at 4 mM (~3× K_m^{ATP}); Rb^{ING} was used as the varied substrate, and staurosporine concentrations were 0 (●), 250 nM (○), and 500 nM (×). C, Rb^{ING} was held constant at 1.8 mM (5× K_m^{Rb^{ING}}), and ATP was used as the varied substrate at ADP concentrations of 0.75 mM (●), 1.5 mM (○), 3 mM (×), and 6 mM (■). See the legend to Fig. 3 for further details.

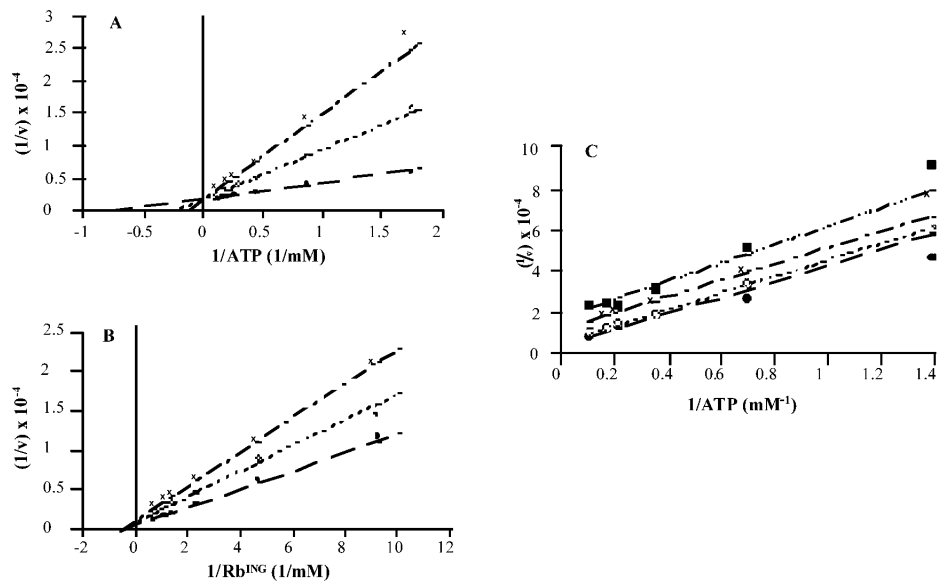
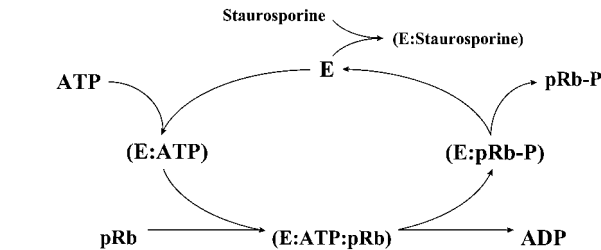


TABLE IV
Inhibition of cyclin D1/CDK4 by staurosporine

Varied substrate	Inhibition mode	Inhibition constant	
		Complex	Fusion
ATP	Competitive	120	137
Rb ^{ING}	Noncompetitive	530	670



SCHEME 1. Proposed kinetic mechanism of cyclin D1-CDK4 (E = cyclin D1-CDK4).

explained above. The results of kinetic experiments followed by the modeling studies will be used to design new inhibitors or modify the existing inhibitors for selectivity and improved binding.

DISCUSSION

As an important target for cell cycle regulation, we have purified the dimeric cyclin D1-CDK4 complex, characterized its essential physical, structural, catalytic, and kinetic properties and established its kinetic mechanism. In addition, for comparison, we have purified the cyclin D1-CDK4 fusion protein and determined its similar kinetic properties and kinetic mechanism. As discussed below, both kinase forms appear complementarily useful in the inhibitor evaluation toward antiproliferative inhibitor discovery.²

The dimeric complex was purified to near-homogeneity by a four-step conventional procedure, whereas the fusion protein containing a six-histidine tag was isolated by a three-step protocol using a metal affinity column as the first step. Western blot, protein mass spectrometry, peptide mapping, and the optimized kinase assay confirmed the molecular/functional identity of both purified forms. From high resolving Mono P and Superdex 200, the complex form was detected as a single activity peak, suggesting that the 67-kDa dimeric enzyme, but not either subunit or

other oligomeric form, is the minimal functional component. An assembly factor (8) does not appear to be required for the kinase activity, even though from the above experimental data it cannot be determined if this factor is needed for proper folding during translational or post-translational modification or otherwise non-functional aggregates may arise. The observation of the dimeric enzyme as a single activity form is supported by a single phosphorylation of the CDK4 subunit and also by the absence of biphasic kinetic behavior at any concentration of the phosphoacceptor substrate (Rb^{ING} or Rb²¹; not shown) during saturation kinetic experiments. During an alternative purification for the complex enzyme, Reactive Green 19 was used as an affinity ligand as the final step after hydroxyapatite. Even though the enzyme was eluted as a homogeneous preparation at 0.8 M NaCl, the activity recovery was very low (~0.2%), and the lost activity was not recovered upon dialysis. We examined the possibility of a direct correlation between the enzyme activity or stability and the ionic strength. At a high ionic strength (e.g. 100 mM Hepes), both the enzyme activity and stability decreased (not shown), probably as a consequence of a change of subunit-subunit interaction mode leading to dissociation in the extreme case. Thus, the low activity recovery for the complex enzyme may be partially attributed to the conformational sensitivity of the heterodimer, which requires both subunits in the right position with respect to each other in order for the enzyme to be fully active (48). This cyclin-CDK interaction is also significant for the sequence recognition of the substrate by the latter subunit. Although the affinity of cyclin H-CDK2,7 and cdc2 complexes has been reported to be in the nanomolar range (48), this did not appear to be the case with the cyclin D1-CDK4 complex since we were unable to reconstitute cyclin D1-CDK4 as an active holoenzyme from its subunits (not shown). On the other hand, the kinase activity of the cyclin D1-CDK4 fusion protein, despite the fact that the enzyme aggregated slowly, appeared to be more stable than the complex enzyme at 4 °C. Most likely, the formation of a functional cyclin D1-CDK4 complex requires the involvement of an assembly factor (8). Also, the low activity recovery may be caused by the microheterogeneity of the protein due to post-translational modifications from the recombinant baculovirus insect cells (41). While a broad activity peak was observed during each one of the first two steps, only the high specific activity portion was further purified in the subsequent steps. Despite the low recovery of the activity, the purified dimeric kinase was highly active and moderately stable.

The kinetic mechanism of the purified cyclin D1-CDK4 com-

TABLE V
Substrate specificity of complex and fusion cyclin D1/CDK4

The same kinase activity was used: complex, 50 μ g; and fusion, 42 μ g.

Peptide (concentration)	Sequence	Complex activity ^a	Fusion activity ^a
Rb 238–259 (1 mg/ml)	PYKTAVIPINGSRPTPRRGQNR	2801	3021
Rb 244–259 (1 mg/ml)	IPINGSRPTPRRGQNR	3943	3712
Rb 246–257 (2 mg/ml)	INGSPRTPRRGQNR ^b	5300	5136
Rb 799–814 (2 mg/ml)	IPGGNIYISPLKSPYK	31	96
Rb 803–815 (2 mg/ml)	NIYISPLKSPYK	100	171
Rb 799–830 (2 mg/ml)	IPGGNIYISPLKSPYKISEGLPTPTKMTTPRSR	451	452

^a The activity was expressed as cpm of [³²P]PO₄ incorporated in the peptide per 30 min.

^b Rb^{ING}.

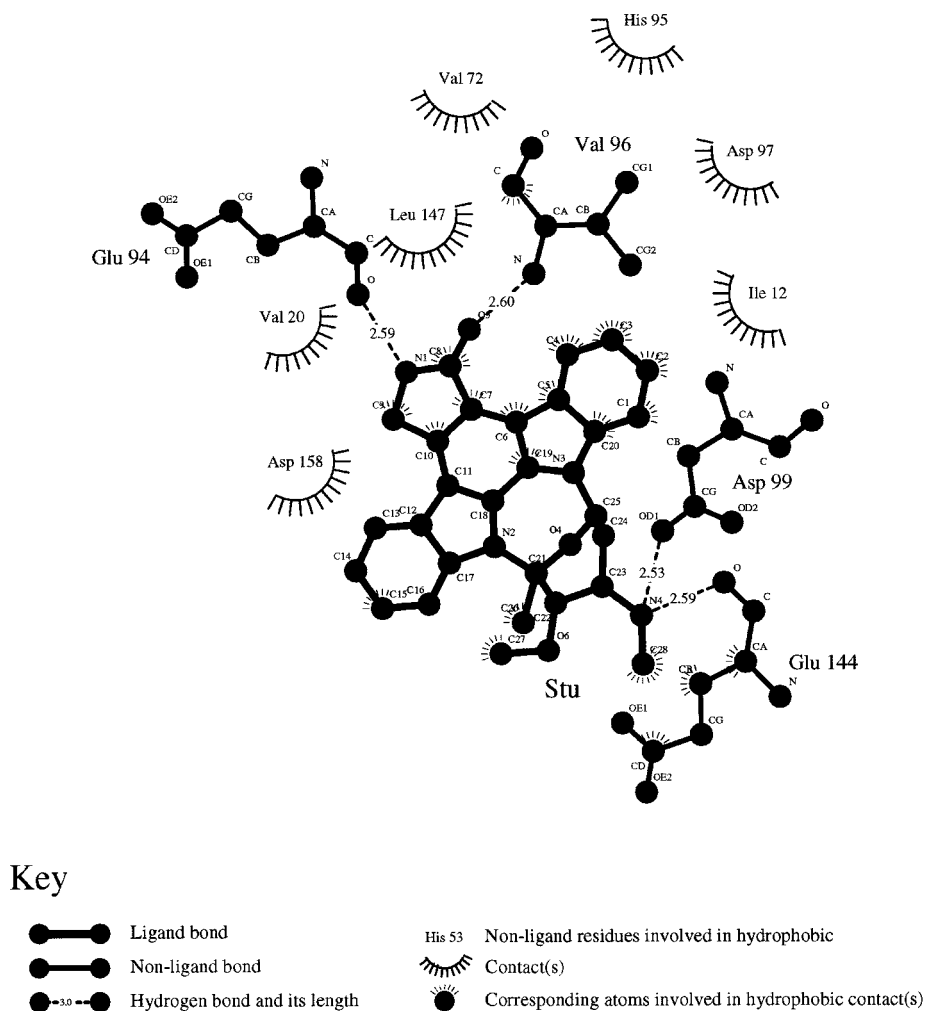
TABLE VI
Cyclin D1/CDK4, kinetic constants of three p^{Rb} peptides

Rb peptide	Sequence	Complex		Fusion	
		V _{max} ^a	K _m ^b	V _{max}	K _m
Rb 605–619	MYLSPVRSPKKKGST	46,540	0.32	41,950	0.36
Rb 782–794	IPHIPRSPYKFPS	23,100	0.33	19,430	0.266
Rb 772–787	PPTLSPIPHIPRSPYK	22,700	1.8	18,000	1.6

^a V_{max} was expressed as cpm of [³²P]PO₄ incorporated in the peptide per 30 min.

^b K_m, mM.

FIG. 5. Interaction of staurosporine with CDK4 at the ATP-binding site.



CDK4 - Staurosporine (Stu)

plex was established using the small peptide Rb^{ING}, the more physiologically relevant protein Rb²¹, and two common kinase inhibitors, staurosporine as a dead-end inhibitor and ADP as a

product inhibitor. Availability of a highly pure, active, and stable kinase in sufficient quantity is an important prerequisite for our detailed structural and functional analyses. The

only confirmed target for cyclin D1-CDK4 is pRb (10), although MyoD has also been suggested to be a target (49). pRb expression and purification were attempted (50)³ in our laboratory, but the yield was not sufficient for any informative kinetic study. The cost of full-length pRb appears prohibitively expensive for a thorough kinetic investigation. Therefore, we examined the kinetic mechanism using the small 12-residue peptide Rb^{ING} containing one phosphorylation site and subsequently examined how these kinetic results were changed when Rb²¹, a more physiologically relevant substrate, was used as the phosphoacceptor. This larger protein is more physiologically relevant since it represents the C terminus (aa 769–921) of full-length pRb (928 aa) and also contains the phosphorylation site Ser-780 which appears to be specific for cyclin D1-CDK4 (5). The C-terminal one-third of the pRb protein contains both the nuclear localization sequences (51) and a DNA binding activity, which to date has not been shown to be specific for any particular DNA sequence (52). The difference in the binding affinity of ATP (130-fold) in the two cases may reflect the significance of the interaction of the enzyme with the phosphoacceptor substrate regarding to the nucleotide binding. Possibly, the phosphoacceptor length plays a critical role in the binding mode of ATP. The interaction of the cyclin D1-CDK4 complex and its phosphoacceptor may be similar or complementary to that achieved by the phosphorylation of the T-loop motif by CAK leading to the activation of the dimeric kinase (48).

When Rb^{ING} was used as the phosphoacceptor substrate, the kinetic mechanism of the dimeric enzyme appeared to be Ordered Bi Bi with Mg²⁺-ATP as the leading substrate and phosphorylated pRb as the last product released, as shown in Scheme 1. The same mechanism was observed for the purified fusion form, and the magnitude of the kinetic parameters was similar (Table III). In this respect, cyclin D1-CDK4 resembles creatine kinase (53), yeast hexokinase (54), and *Escherichia coli* galactokinase (55) rather than nucleotide diphosphate kinase which has a ping-pong mechanism with a stable phosphoenzyme intermediate (24). Also, a comparison of cyclin D1-CDK4 with other kinases for staurosporine inhibition is of great interest (43). The competitive inhibition pattern of cyclin D1-CDK4 obtained with staurosporine with respect to ATP has also been observed with cAMP-dependent protein kinase A, casein kinase 2, angiotensin II, as well as mitogen-activated protein kinase extracellular receptor kinase-1, c-Src kinase, tyrosine kinase-IIB/p38, and epidermal growth factor receptor kinase (43). According to this report, in contrast to the ATP-staurosporine competitive pattern, the phosphoacceptor substrate exhibits kinetics with respect to staurosporine that are different depending on the residue specificity (Ser/Thr or Tyr) of the kinase (43). So, the kinetic experiments with respect to varied phosphoacceptor-substrate concentrations (44), at constant ATP, support a pattern of uncompetitive inhibition in the case of protein-Ser/Thr kinase and non-competitive inhibition for protein-Tyr kinase. Thus, as a Ser/Thr-specific protein kinase, cyclin D1-CDK4 appears not to follow this trend and operates by a non-competitive inhibition mechanism (Fig. 4).

When Rb²¹ was used as the phosphoacceptor substrate, the binding parameter (K_m) of the dimeric complex to ATP increased 130-fold. This tighter binding is expected since the larger Rb²¹ can assume a tertiary structure possessing more extended interactions that could induce a conformational change in the enzyme thus lowering the K_m toward ATP. Although the exact affinity constant of Rb²¹ was not determined because of our inability to reach saturation concentration of the phosphoacceptor, a similar effect for tight binding of the en-

zyme complex to the phosphoacceptor was also observed (not shown). Interestingly, ATP substrate inhibition was observed at a concentration higher than $5 \times K_m$ with Rb^{ING} but not with Rb²¹ (up to $40 \times K_m$), in agreement with an Rb²¹-induced conformational change of the dimeric complex which permits productive binding of the ATP substrate. Thus the establishment of the kinase assay with both the small peptide Rb^{ING} and the more physiologically relevant Rb²¹ appears essential in large scale inhibitor screening evaluation for the mode and the magnitude of the kinase-inhibitor interaction.

To improve the understanding of the inhibitor binding in the ATP-binding site, we attempted to model staurosporine using CDK2-staurosporine as a template since both kinases share a very high sequence similarity. A number of interesting interactions between the protein and the inhibitor were identified that qualitatively support the magnitude of affinity between cyclin D1-CDK4 and staurosporine and further substantiates our kinetic inhibition mechanism. We anticipate that the combinatorial application of the kinetic and inhibition data as well as the modeling of any novel inhibitors in the active site could be useful in discovery of potent inhibitors with anti-tumor activity.

In summary, we have purified the cyclin D1-CDK4 complex, confirmed it as the active dimeric enzyme, developed an optimal *in vitro* assay, and established its kinetic mechanism. We have also purified and analyzed the cyclin D1-CDK4 fusion protein, which showed similar kinetic properties and the same kinetic mechanism to the dimeric complex and thus validated the cell-based assay.² In addition, we have initiated an effort to elucidate the crystal structure of the kinase (as dimeric complex or fusion protein). We anticipate that the dimeric enzyme and its *in vitro* assay as well as fusion protein and the cell-based assay (where the cell lines depended on the fusion protein for growth) can be synergistically useful in the antiproliferative drug discovery.

Acknowledgments—We thank Steve Kovacevic, Cheryl Kussow, Tony Sheppard, Jim Miller, Nancy Rankl, and Keith Houck for providing all baculovirus-infected insect cells; Jeff Dixon, Duane Bronson, and Warren MacKellar for assistance in the initial purification of the complex enzyme; Jeff Larsen for gene expression of pRb and Sandhya Ghag for pRb purification; members of the Cell Cycle Action Group for helpful suggestions; Mel Johnson for protein/peptide sequencing; Jon Butler for peptide synthesis; John Richardson for assistance in protein mass spectrometry; Gerald Becker and John Hale for advice in protein structural characterization; and Richard Schevitz for crystallographic discussion. We are also grateful to Bill Heath for managerial support.

REFERENCES

- Wang, J. Y., Knudsen, E. S., and Welch, P. J. (1994) *Adv. Cancer Res.* **64**, 25–85
- Lukas, J., Parry, D., Aagaard, L., Mann, D. J., Bartkova, J., Strauss, M., Peters, G., and Bartek, J. (1995) *Nature* **375**, 503–506
- Dynlacht, B. D., Flores, O., Lees, J. A., and Harlow, E. (1994) *Genes Dev.* **8**, 1772–1786
- Suzuki-Takahashi, I., Kitagawa, M., Saijo, M., Higashi, H., Ogino, H., Matsumoto, H., Taya, Y., Nishimura, S., and Okuyama, A. (1995) *Oncogene* **10**, 1691–1698
- Kitagawa, M., Higashi, H., Jung, H.-K., Suzuki-Takahashi, I., Ikeda, S., Tamai, K., Kato, J., Segawa, K., Yoshida, E., Nishimura, S., and Taya, Y. (1996) *EMBO J.* **15**, 7060–7069
- Helin, K., and Harlow, E. (1993) *Trends Cell Biol.* **3**, 43–46
- Sherr, C. J. (1994) *Cell* **79**, 551–554
- Stepanova, L., Leng, X., Parker, S. B., and Harper, J. W. (1996) *Genes Dev.* **10**, 1491–1502
- Morgan, D. O. (1995) *Nature* **374**, 131–134
- Elledge, S. J., and Harper, J. W. (1994) *Curr. Opin. Cell Biol.* **6**, 847–852
- Sherr, C. J., and Roberts, J. M. (1995) *Genes Dev.* **9**, 1149–1163
- Patra, D., and Dunphy, W. G. (1996) *Genes Dev.* **10**, 1503–1515
- Taya, Y., Yasuda, H., Kamijo, M., Nakaya, K., Nakamura, Y., Ohba, Y., and Nishimura, S. (1989) *Biochem. Biophys. Res. Commun.* **164**, 580–586
- Lees, J. A., Buchkovich, K. J., Marshak, D. R., Anderson, C. W., and Harlow, E. (1991) *EMBO J.* **10**, 4279–4290
- Hamel, P. A., Gill, R. M., Phillips, R. A., and Gallie, B. L. (1992) *Oncogene* **7**, 693–701
- Mittnacht, S., Lees, J. A., Desai, D., Harlow, E., Morgan, D. O., and Weinberg, R. A. (1994) *EMBO J.* **13**, 118–127

³ S. K. Ghag and W. K. Yeh, unpublished data.

17. Knudsen, E. S., and Wang, J. Y. (1997) *Mol. Cell. Biol.* **17**, 5771–5783
18. Zarkowska, T., and Mittnacht, S. (1997) *J. Biol. Chem.* **272**, 12738–12746
19. Connell-Crowley, L., Harper, J. W., and Goodrich, D. W. (1997) *Mol. Biol. Cell* **8**, 287–301
20. Zarkowska, T., U, S., Harlow, E., and Mittnacht, S. (1997) *Oncogene* **14**, 249–254
21. Lunberg, A. S., and Weinberg, R. A. (1998) *Mol. Cell. Biol.* **18**, 753–761
22. Cordon-Cardo, C. (1995) *Am. J. Pathol.* **147**, 545–560
23. Karp, J. E., and Broder, S. (1995) *Nat. Med.* **1**, 309–320
24. Mourad, N., and Parks, R. E., Jr. (1966) *J. Biol. Chem.* **241**, 271–278
25. Kitagawa, M., Saitoh, S., Ogino, H., Okabe, T., Matsumoto, H., Okuyama, A., Tamai, K., Ohba, Y., Yasuda, H., and Nishimura, S. (1992) *Oncogene* **7**, 1067–1074
26. Higashi, H., Suzuki-Takahashi, I., Taya, Y., Segawa, K., Nishimura, S., and Kitagawa, M. (1995) *Biochem. Biophys. Res. Commun.* **216**, 520–525
27. Rice, J. W., Rankl, N. B., Gurganus, T. M., Marr, C. M., Barna, J. B., Walters, M. M., and Burns, D. J. (1993) *BioTechniques* **15**, 1052–1059
28. Otto, K. A., Kovacevic, S. A., Lemke, S. J., Cocke, K., Beckmann, R. P., and Rao, R. N. (1996) *Keystone Symposium on Molecular and Cellular Biology, Silverthorne, CO, Jan. 11–17, 1996*, Abstr. 338
29. Whitaker, J. R., (1963) *Anal. Chem.* **35**, 1950–1953
30. Segel, I. H., (1993) *Enzyme Kinetics, Behavior and Analysis of Rapid Equilibrium and Steady State Enzyme Kinetics*, pp. 505–845, John Wiley & Sons, New York
31. Greer, J. (1980) *Proc. Natl. Acad. Sci. U. S. A.* **77**, 3393–3397
32. Greer, J. (1990) *Proteins* **7**, 317–334
33. Zheng, J., Knighton, D. R., ten Eyck, L. F., Karlsson, R., Xuong, N., Taylor, S. S., and Sowadski, J. M. (1993) *Biochemistry* **32**, 2154–2161
34. Zhang, F., Strand, A., Robbins, D., Cobb, M. H., and Goldsmith, E. J. (1994) *Nature* **367**, 704–711
35. Lawrie, A. M., Noble, M. E., Tunnah, P., Brown, N. R., Johnson, L. N., and Endicott, J. A. (1997) *Nat. Struct. Biol.* **4**, 796–801
36. Bernstein, F. C., Koetzle, T. F., Williams, G. J., Meyer, E. E., Jr., Brice, M. D., Rodgers, J. R., Kennard, O., Shimanouchi, T., and Tasumi, M. (1977) *J. Mol. Biol.* **112**, 535–542
37. Sali, A., and Blundell, T. L. (1993) *J. Mol. Biol.* **234**, 779–815
38. Nobuyuki, F., Hiroaki, T., Yaeko, K., Yumiko, T., Yoshihiro, H., Yuzuru, I., and Satoshi, O. (1994) *Tetrahedron Lett.* **35**, 1251–1254
39. Furet, P., Caravatti, G., Lydon, N., Priestle, J. P., Sowadski, J. M., Trinks, U., and Traxler, P. (1995) *J. Comput. Aided Mol. Des.* **9**, 465–472
40. Brooks, B. R., Bruccoleri, R. E., Olafson, B. D., States, D. J., Swaminathan, S., and Karplus, M. (1983) *J. Comp. Chem.* **4**, 187–217
41. Churgay, L. M., Rankl, N. B., Richardson, J. M., Becker, G. W., and Hale, J. E. (1997) in *Techniques in Protein Chemistry* (Marshak, D. R., ed) pp. 837–849, Academic Press, New York
42. Wood, H. G., Davis, J. J., and Lochmuller, H. (1966) *J. Biol. Chem.* **241**, 5692–5704
43. Meggio, F., Donella Deana, A., Ruzzene, M., Brunati, A. M., Cesaro, L., Guerra, B., Meyer, T., Mett, H., Fabbro, D., Furet, P., Dobrowolska, G., and Pinna, L. A. (1995) *Eur. J. Biochem.* **234**, 317–322
44. Lin, B. T.-Y., Gruenwald, S., Morla, A. O., Lee, W.-H., and Wang, J. Y. J. (1991) *EMBO J.* **10**, 857–864
45. Jeffrey, P. D., Russo, A. A., Polyak, K., Gibbs, E., Hurwitz, J., Massague, J., and Pavletich, N. P. (1995) *Nature* **376**, 313–320
46. Wallace, A. C., Laskowski, R. A., and Thornton, J. M. (1996) *Protein Sci.* **5**, 1001–1013
47. Smith, T. F., and Waterman, M. S. (1981) *J. Mol. Biol.* **147**, 195–197
48. Heitz, F., Morris, M. C., Fesquet, D., Cavadore, J.-C., Doree, M., and Divita, G. (1997) *Biochemistry* **36**, 4995–5003
49. Skapek, S. X., Rhee, J., Spicer, D. B., and Lassar, A. B. (1995) *Science* **267**, 1022–1025
50. Hensey, C. E., Hong, F., Durfee, T., Quian, Y.-W., Lee, E. Y.-H. P., and Lee, W.-H. (1994) *J. Biol. Chem.* **269**, 1380–1387
51. Shew, J.-Y., Lin, B. T.-Y., Chen, P. L., Tseng, B. Y., Yang-Feng, T. L., and Lee, W.-H. (1990) *Proc. Natl. Acad. Sci. U. S. A.* **87**, 6–10
52. Wang, N.-P., Qian, Y., Chung, A. E., Lee, W.-H., and Lee, E. Y.-H. P. (1990) *Cell Growth Differ.* **1**, 233–239
53. Morrison, J. F., and James, E. (1965) *Biochem. J.* **97**, 37–42
54. Hammes, G. G., and Kochavi, D. (1962) *J. Am. Chem. Soc.* **84**, 2069–2073
55. Gulbinski, J. S., and Cleland, W. W. (1968) *Biochemistry* **7**, 566–575